Biomaterials Science

ROYAL SOCIETY OF CHEMISTRY

PAPER

View Article Online
View Journal

Cite this: DOI: 10.1039/d1bm00223f

Open-air synthesis of oligo(ethylene glycol)-functionalized polypeptides from non-purified *N*-carboxyanhydrides†

Zhengzhong Tan,‡[a] Ziyuan Song, ‡[a] Tianrui Xue,[b] Lining Zheng,[a] Lei Jiang,[a,c] Yunjiang Jiang, [a] Zihuan Fu,[b] Anh Nguyen,[d] Cecilia Leal [a] and Jianjun Cheng *[a,b,e,f,g]

Received 7th February 2021,
Accepted 7th April 2021

DOI: 10.1039/d1bm00223f

rsc.li/biomaterials-science

With PEG-like properties, such as hydrophilicity and stealth effect against protein absorption, oligo(ethylene glycol) (OEG)-functionalized polypeptides have emerged as a new class of biomaterials alternative to PEG with polypeptide-like properties. Synthesis of this class of materials, however, has been demonstrated very challenging, as the synthesis and purification of OEG-functionalized *N*-carboxyanhydrides (OEG-NCAs) in high purity, which is critical for the success in polymerization, is tedious and often results in low yield. OEG-functionalized polypeptides are therefore only accessible to a few limited labs with expertise in this specialized NCA chemistry and materials. Here, we report the controlled synthesis of OEG-functionalized polypeptides in high yield directly from the OEG-functionalized amino acids *via* easy and reproducible polymerization of non-purified OEG-NCAs. The prepared amphiphilic block copolypeptides can self-assemble into narrowly dispersed nanoparticles in water, which show properties suitable for drug delivery applications.

Introduction

Oligo(ethylene glycol) (OEG)-functionalized polypeptides are emerging new biomaterials with both poly(ethylene glycol) (PEG)- and peptide-like properties.[1] Resembling the functions of PEG in biomaterials, the OEG-functionalized polypeptide segments provide excellent water-solubility and satisfactory resistance to protein binding. Therefore they can potentially be used as the components of drug delivery vehicles,[2–4] the hydrophilic structural motifs of block copolymers for self-assembly,[5–7] and the building blocks of hydrogels for tissue engineering.[8–10] On the other hand, the OEG-functionalized polypeptides adopt stable secondary structures due to their peptide backbones, which endow new functions that are not observed for conventional, random-coiled polymers.[11,12] For example, the incorporation of non-ionic, hydrophilic OEG to helical polypeptides enables superior stealth effect to prevent protein binding,[13,14] reduced *in vivo* immunogenicity,[15] tunable thermo-responsiveness,[16–18] and capability of forming non-covalent polypeptide hydrogels.[17,19] Deming and coworkers were the first to report the design and synthesis of the OEG-functionalized polypeptides and demonstrated their excellent water-solubility and helical stability.[20] Li and coworkers later reported the lower critical solution temperature (LCST) property of such materials.[16,21,22] Recently, Lu and coworkers demonstrated that the conjugates of protein therapeutics with the OEG-functionalized polypeptides achieved improved circulation half-life and reduced immune response compared to PEG-protein conjugates, substantiating the advantages of these materials over PEG in drug delivery,[15] in particular with the growing concern of immunogenicity with the extensive use of PEG.[23,24]

The preparation of OEG-functionalized polypeptides, however, is difficult even to an experienced chemist. Synthesis of such polypeptides are typically through the ring-opening polymerization of OEG-functionalized amino acid *N*-carboxyanhydrides (OEG-NCAs).[14,16,20,21] NCAs are moisture-sensitive and therefore typically handled under inert-gas protection and anhydrous condition.[25,26] The conventional monophasic polymerization, typically in *N*,*N*-dimethylformamide (DMF), requires NCA monomers in very high purity, which

[a]*Department of Materials Science and Engineering, University of Illinois at Urbana-Champaign, Urbana, Illinois 61801, USA. E-mail: jianjunc@illinois.edu*
[b]*Department of Chemistry, University of Illinois at Urbana-Champaign, Urbana, Illinois 61801, USA*
[c]*State Key Laboratory of Natural Medicines, Department of Pharmaceutics, China Pharmaceutical University, Nanjing 210009, China*
[d]*Department of Chemical and Biomolecular Engineering, University of Illinois at Urbana-Champaign, Urbana, Illinois 61801, USA*
[e]*Beckman Institute for Advanced Science and Technology, University of Illinois at Urbana-Champaign, Urbana, Illinois 61801, USA*
[f]*Department of Bioengineering, University of Illinois at Urbana-Champaign, Urbana, Illinois 61801, USA*
[g]*Materials Research Laboratory, University of Illinois at Urbana-Champaign, Urbana, Illinois 61801, USA*
†Electronic supplementary information (ESI) available. See DOI: 10.1039/d1bm00223f
‡These authors contributed equally.

otherwise would not proceed or yield poorly controlled polypeptides.[27] NCAs in high purity are typically achieved through multiple recrystallizations[20] or by flash column separation under inert-gas protection.[21] The recrystallization process is very challenging to OEG-NCAs due to their poor crystallinity, and often results in oily residues containing many impurities.[28] Preparation of high-purity OEG-NCAs suitable for polymerization requires special experience with this class of molecules and often leads to suboptimal or very low yield, even to an experienced NCA chemist. It is therefore not surprising that OEG-functionalized polypeptides were reported and used by only a very small number of research groups because of its difficulty of synthesis and limited availability to non-experts.

We attempted the possibility of controlled polymerization with non-purified OEG-NCAs, avoiding the tedious purification steps of the monomers. To achieve this goal, we reasoned that the impurities of OEG-NCAs need to be segregated in order not to interfere with the polymerization process. Inspired by the efficient amide bond formation during the protein translation process in ribosome, which is made possible under "open" conditions mainly because of two intrinsic features: firstly, fast catalyzed reaction outpaces side reactions such as hydrolysis; secondly, water and other hydrophilic molecules are segregated from the reaction site, facilitating the peptide bond formation.[29–31] Our group recently reported a biomimetic biphasic polymerization strategy namely Segregation-Induced Monomer-Purification and initiator-Localization promoted rate-Enhancement (SIMPLE).[32] This SIMPLE polymerization strategy enables the *in situ* purification of non-purified NCAs by segregating hydrophilic impurities into water, promoting the polymerization of NCAs in the organic phase at an ultrafast kinetics, which was enabled by α-helical macromolecular initiators that outpaces water-induced NCA degradation. Recently, our group further reported the fast polymerization kinetics of NCA by α-helical macromolecular initiators when catalyzed by crown ether (CE) which enhances the NCA/polypeptide interaction by binding with the terminal amine of the growing polypeptide chain and the N–H of the NCA monomer.[33]

Here, we report the controlled polymerization of γ-(2-(2-(2-methoxyethoxy) ethoxy) ethoxy)-esteryl-L-glutamate NCA (EG_3Glu-NCA) using SIMPLE polymerization that does not require sophisticated, inert-gas-protected purifications (*i.e.*, recrystallization or column separation) of NCAs. The brownish, "dirty" NCA from the phosgenation of EG_3Glu was directly used for the polymerization, which proceeds in a water/$CHCl_3$ biphasic system with a helical poly(N_ε-carboxybenzyl-L-lysine) (PZLL) initiator and a CE catalyst. A variety of OEG-functionalized polypeptides were obtained with high molecular weights, low dispersity ($Đ$ < 1.2) and excellent isolated yields (>50%), demonstrating the SIMPLE polymerization strategy can purify and polymerize not only hydrophobic NCAs, but also water-soluble OEG-NCAs. The amphiphilic block copolypeptides with the OEG-functionalized polypeptide segment could readily self-assemble into nanoparticles in aqueous environment, encapsulating model drug (paclitaxel (PTX)) with 11% loading content.

Results and discussion

Non-purified EG_3Glu-NCA

EG_3Glu-NCA monomers were prepared as previously reported.[21] In brief, esterification reaction was used to conjugate the monomethylated triethylene glycol onto the γ-carboxylic acid group of L-glutamic acid. The EG_3Glu-NCA was synthesized through phosgenation, the so-called Fuchs-Farthing method (Scheme 1). Due to the poor crystallinity, it is difficult to purify EG_3Glu-NCA using traditional recrystallization method. Several groups reported the successful purification of EG_3Glu-NCA by anhydrous silica chromatography, with the purified monomer obtained as a colorless oil.[21] In this study, we attempted to directly polymerize non-purified EG_3Glu-NCA, which is a brownish oil (Scheme 2) obtained by precipitation of reaction mixture with hexane followed by the removal of solvent *in vacuo*. Besides the obvious difference in color as compared to clean EG_3Glu-NCA, the existence of impurities in the non-purified EG_3Glu-NCA was also confirmed by the elemental analysis. It was showed that the non-purified EG_3Glu-NCA has ~1 wt% of chlorine, originating from halide-containing impurities during NCA synthesis.[28]

As the biphasic system is to *in situ* purify NCA during the polymerization, we explored the partition of EG_3Glu-NCA in the water and oil phases. A water/chloroform biphasic system was prepared by adding water to the chloroform solution of EG_3Glu-NCA, which mimicked the polymerization conditions ($[NCA]_0$ = 17 mM, water : chloroform = 3 : 25, v/v). FTIR characterization showed that 89% of EG_3Glu-NCA remained in the $CHCl_3$ phase after 2.5 h after mixing with water, confirming the feasibility of direct polymerization of EG_3Glu-NCA in the presence of aqueous phase (Fig. 1a and Fig. S1†).

Polymerization of OEG-NCA

Protein synthesis takes places in a complex supramolecular machine, ribosome, through the rapid amidation chemistry that outpaces other competing side reactions, in particular the hydrolysis reaction. As demonstrated in our previous study, reversible binding between the N-terminus of α-helical poly-

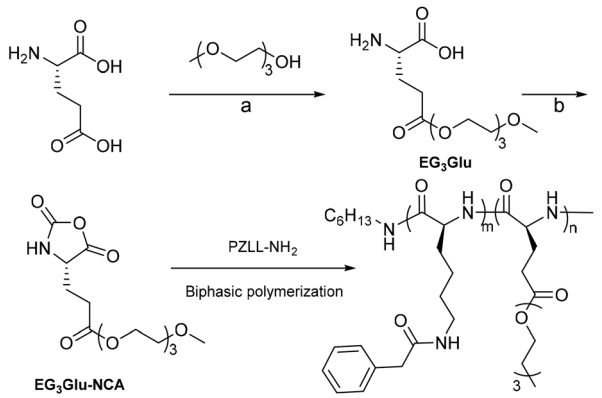

Scheme 1 Synthesis routes to EG_3Glu-NCA and OEG-functionalized polypeptides. (a) H_2SO_4, 0 °C to rt, overnight; (b) phosgene, 50 °C, 2 h.

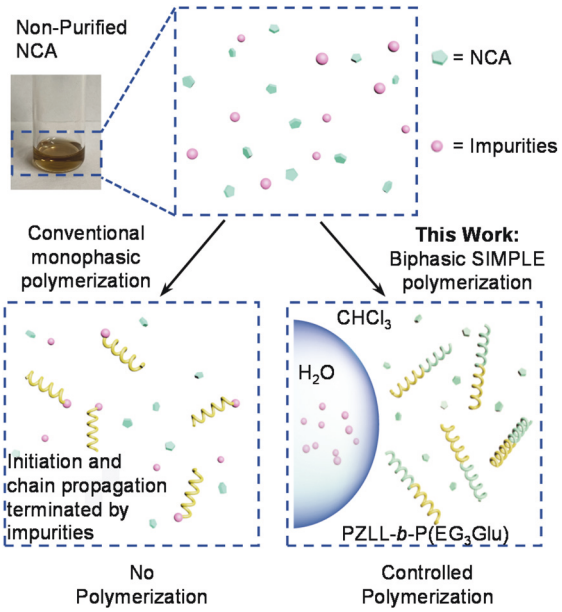

Scheme 2 Illustration of conventional monophasic polymerization (left) *vs.* the biphasic polymerization (right) of non-purified EG_3Glu-NCA. In conventional monophasic polymerization, the initiator (yellow) was quenched by impurities (red), preventing polymerization from happening, while in the biphasic polymerization, the impurities were extracted in the water droplet (blue) in the biphasic system, enabling the OEG-grafted NCAs (light green) to be polymerized by the α-helical macromolecular initiator.

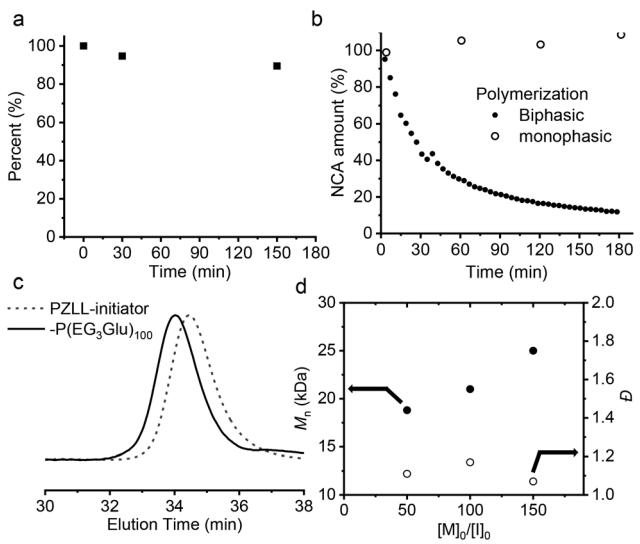

Fig. 1 (a) Percentage of remaining EG_3Glu-NCA in $CHCl_3$ phase after mixing with water (water : chloroform = 3 : 25, v/v) as determined by FTIR. (b) NMR study of polymerization kinetics of non-purified EG_3Glu-NCA in monophasic and biphasic system. (c) GPC curves (LS signal) of PZLL initiator and $PZLL_{45}$-*b*-$P(EG_3Glu)_{100}$. (d) Molecular weight (filled circle) and dispersity (open circles) of resulting polypeptides from SIMPLE polymerization of non-purified EG_3Glu-NCA using PZLL initiator with different $[M]_0/[I]_0$ ratio. $[NCA]_0$ = 17 mM, $[M]_0/[I]_0$ = 50, 100, and 150.

peptides and NCA promotes rate acceleration of the subsequent ring-opening reaction, following the typical Michaelis–Menten-type enzymatic kinetic model.[34] We therefore tested the use of a preformed α-helical PZLL bearing terminal amino group ($PZLL\text{-}NH_2$, DP = 41) as the initiator. It is well known that even trace amount of impurities would impair the polymerization of NCAs in DMF, chloroform, or dichloromethane (DCM) monophasic system, which was confirmed to be the case for our non-purified EG_3Glu-NCA. $PZLL\text{-}NH_2$-initiated polymerization of non-purified EG_3Glu-NCA in chloroform-d ($CDCl_3$), as monitored by ^1H NMR, showed no reaction of NCA after 3 h, presumably due to the quenching of the amino initiators by various acidic or acyl impurities. In sharp contrast, non-purified EG_3Glu-NCA was rapidly polymerized by $PZLL\text{-}NH_2$ in the presence of aqueous phase under identical condition, resulting in 70% consumption of EG_3Glu-NCA within 1 h, as monitored by ^1H NMR (Fig. 1b). The fast polymerization kinetics was also validated by monitoring the change of the peak intensity at 1793 cm^{-1} (*i.e.*, anhydride peak from NCA) with FTIR, which showed that the EG_3Glu-NCA was largely consumed in 50 min (Fig. S2†). The role of CE on polymerization kinetics was also investigated using NMR. Compared to ~70% NCA consumption in 1 h under CE catalysis, less than ~30% NCA was consumed in 1 h without CE catalysis, showing that CE can greatly increase the polymerization rate (Fig. S3†). These experiments demonstrated that biphasic system could effectively purify the non-purified EG_3Glu-NCA *in situ*, avoiding otherwise much more complicated purifications, and enables the successful ring-opening reaction of the non-purified EG_3Glu-NCA.

OEG-functionalized co-polypeptides

After demonstrating the feasibility of polymerizing non-purified EG_3Glu-NCA, we next explored if the polymerization in the biphasic system condition could allow control over molecular weights of the resulting EG_3Glu polypeptides. Non-purified EG_3Glu-NCA at different $[M]_0/[I]_0$ ratios (*i.e.*, 50, 100, and 150) was polymerized by biphasic polymerization using $PZLL\text{-}NH_2$ as the initiator. The resulting polypeptides showed monomodal GPC peaks and narrow dispersity ($Đ$ < 1.2, Fig. 1d; entries 1–3, Table 1), indicating well-controlled polymerization process. Moreover, the obtained MW can be tuned by changing the $[M]_0/[I]_0$ ratios (Fig. 1c and Fig. S4†), with larger MW observed at higher $[M]_0/[I]_0$ ratio. However, at high $[M]_0/[I]_0$ (*i.e.*, $[M]_0/[I]_0$ = 150), the obtained MW of polypeptides was smaller than the expected MW, likely due to the longer polymerization time that the water-induced degradations of NCAs became more significant. The resulting block copolypeptides adopted an α-helical secondary structure as characterized by CD (Fig. S5†), which was demonstrated to be crucial in the non-fouling property of OEG-grafted polypeptides.[15]

To further demonstrate the robustness of the polymerization, $PBLG\text{-}NH_2$ (DP = 44) was used to initiate non-purified EG_3Glu-NCA polymerization using SIMPLE polymerization. The GPC characterization of resulting block copolypeptides confirmed that SIMPLE polymerization of non-purified

Table 1 Characterization of block copolypeptides bearing OEG-functionalized segments[a]

Entry	Polypeptides	$[M]_0/[I]_0$	$M_n/M_n^{*b,c}$ (kDa)	$Đ^c$
1	PZLL-*b*-P(EG_3Glu)	50	18.8/24.6	1.11
2	PZLL-*b*-P(EG_3Glu)	100	21.0/38.4	1.17
3	PZLL-*b*-P(EG_3Glu)	150	25.0/52.1	1.07
4[d]	PZLL-*b*-P(EG_3Glu)-*b*-PBLG	50/50	34.0/36.4	1.18
5[d]	PZLL-*b*-P(EG_3Glu)-*b*-PBLG-*b*-P(EG_3Glu)	50/50/50	40.8/50.1	1.16

[a] Polymerizations were conducted at room temperature in a water/chloroform biphasic system initiated by PZLL-NH_2 initiator. [b] Obtained MW (kDa)/designed MW* (kDa). [c] Determined by GPC. [d] Block copolymerization by the sequential addition of monomers.

EG_3Glu-NCA was widely applicable to many helical macromolecular initiators (Fig. S6†). Moreover, several multi-block copolypeptides were synthesized *via* the sequential addition of non-purified EG_3Glu-NCA and purified BLG-NCA or ZLL-NCA, evidenced by the GPC analysis and low dispersity of the resulting multi-block copolypeptides (Fig. S7;† entries 4 and 5, Table 1). Due to the fast kinetics of polymerization, the active amino group at the end of the growing chain was conserved, making it possible to prepare well-controlled multiblock copolypeptides.[35] Tetra block copolypeptides with alternating hydrophilic and hydrophobic segments were prepared with the use of the non-purified EG_3Glu-NCA.

Self-assembly of OEG-functionalized co-polypeptides

We next tested if the resulting amphiphilic block copolypeptides could be used in self-assembly to form well-defined nanostructures. Given the PEG-like properties previously reported, we explored the formation of nanoparticles with surface-coated P(EG_3Glu). Nanoparticles from $PZLL_{45}$-*b*-P($EG_3Glu)_{50}$, $PZLL_{45}$-*b*-P($EG_3Glu)_{100}$, and $PZLL_{45}$-*b*-P($EG_3Glu)_{150}$ block copolypeptides were formulated using the nanoprecipitation method,[36] with the obtained size of 125.5 nm, 95.7 nm, and 64.6 nm, respectively. Low particle dispersity was observed for all three copolymers (PDI < 0.18, Fig. 2a). TEM and cryo-TEM experiments were also performed to further analyze and confirm the formation of nanoparticles (Fig. 2b and Fig. S8, S9†), showing a spherical morphology with size well correlated with the DLS results. The prepared multiblock polypeptides also could readily form narrowly-dispersed nanoparticles, with a trend of larger size with increasing block numbers (Fig. S10†). Furthermore, when cultured in serum-containing media, none of the nanoparticles showed significant aggregation in 24 h, as no obvious increase of the particle size was observed from the size-intensity graph in DLS test, suggesting its outstanding non-fouling property (Fig. 2c and Fig. S11†). As the serum stability of the nanoparticles is a common challenge to nanoparticles due to their aggregation in blood,[37] and nanoparticles with unsatisfactory PEG density may not completely avoid salt-induced self-aggregation, the high serum stability of the OEG-grafted polypeptides nanoparticle makes them favorable to be used

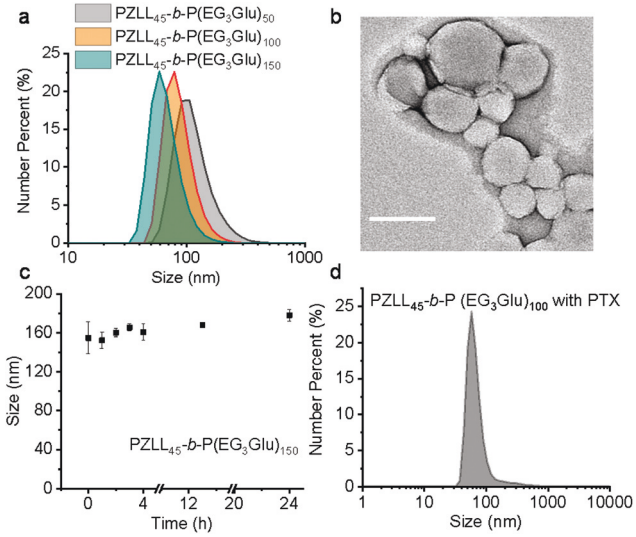

Fig. 2 (a) DLS characterization of nanoparticles formed by $PZLL_{45}$-*b*-P($EG_3Glu)_{50}$, $PZLL_{45}$-*b*-P($EG_3Glu)_{100}$, and $PZLL_{45}$-*b*-P($EG_3Glu)_{150}$ in water. (b) TEM image of $PZLL_{45}$-*b*-P($EG_3Glu)_{150}$ nanoparticles, scale bar = 100 nm. (c) Serum stability of $PZLL_{45}$-*b*-P($EG_3Glu)_{150}$ nanoparticles by DLS characterization of nanoparticles mixed with DMEM media with 10% FBS. The intensity dots represent the size of the peak of nanoparticle in size-intensity diagraph. Error bar represents the standard deviation from three independent tests. (d) DLS characterization of PTX-loaded $PZLL_{45}$-*b*-P($EG_3Glu)_{100}$ nanoparticle.

as a drug delivery vehicle. Encouraged by the well-defined structures and the excellent serum stability of OEG-polypeptide-based nanoparticles, we next explored the use of nanoparticles as drug carriers. PTX-loaded nanoparticles were prepared using nanoprecipitation method by addition of a DMF solution of $PZLL_{45}$-*b*-P($EG_3Glu)_{100}$ and PTX to water. With a decent loading content of 11.2%, the PTX-loaded nanoparticles showed low dispersity and sub-100 nm particle size (size = 76 nm, PDI = 0.28, Fig. 2d), in the size range suitable for drug delivery.[38,39] The cumulative release of PTX from PTX-loaded nanoparticles was tested by dialysis against water. The PTX-loaded $PZLL_{45}$-*b*-P($EG_3Glu)_{100}$ nanoparticles showed no burst release of PTX in at least 24 h (Fig. S12†), in contrast to the undesired burst release of drug typically in PEG-PLA or PEG-PLGA nanoparticles.[40] These data collectively demonstrate the potential of OEG-grafted polypeptide nanoparticle in the drug delivery field.

Experimental

Materials

All chemicals were purchased from MilliporeSigma (St Louis, MO, USA). Amino acids were purchased from Chem-Impex Inc. (Wood Dale, IL, USA). Dialysis membrane was purchased from Repligen Corporation (Waltham, MA, USA). Anhydrous DMF was treated with isocyanate beads (MilliporeSigma, St Louis, MO, USA) in order to remove any nucleophilic impurities and stored in argon-filled glovebox. Anhydrous hexane and THF

were dried in a column using alumina. Anhydrous chloroform and DCM were dried using anhydrous sodium sulfate.

Instrumentation

^{1}H and ^{13}C NMR spectra were obtained on a Varian U500 spectrometer in the NMR laboratory, University of Illinois at Urbana-Champaign. The chemical shifts of the spectra were referenced to the solvent proton and recorded in ppm. Gel permeation chromatography (GPC) characterizations were carried out on an instrument installed with an isocratic pump (1260 Infinity II, Agilent, Santa Clara, CA, USA), a differential refractometer (dRI) detector (Optilab T-rEX, Wyatt Technology, Santa Barbara, CA, USA), and a multi-angle light scattering (MALS) detector with the detection wavelength at 658 nm (DAWN HELEOS-II, Wyatt Technology, Santa Barbara, CA, USA). Separations were performed using serially connected size exclusion columns (three PLgel MIXED-B columns, 10 μm, 7.5 × 300 mm, Agilent, Santa Clara, CA, USA) using DMF with 0.1 M LiBr at 40 °C as the mobile phase at a flow rate of 0.7 mL min^{-1}. The MALS detector was calibrated using pure toluene and can be used for the determination of the absolute molecular weights (MWs). All sample solutions were filtered using a 0.45 μm PTFE filter before injection. The dn/dc value of each sample was calculated offline by using the internal calibration system processed by the ASTRA 7 software (version 7.1.3.15, Wyatt Technology, Santa Barbara, CA, USA) and was used to determine the MWs of polypeptides. Lyophilization was performed on a FreeZone lyophilizer (Labconco, Kansas City, MO, USA). Dynamic Light Scattering (DLS) were performed on a Malvern Zetasizer in Materials Research Laboratory, University of Illinois at Urbana-Champaign. Transmission electron microscopy (TEM) and cryogenic TEM (cryo-TEM) images were obtained using JEOL 2100 cryo transmission electron microscope. Infrared spectra were recorded on a PerkinElmer 100 serial FTIR spectrophotometer calibrated with polystyrene film (PerkinElmer, Santa Clara, CA, USA). Fluorescent spectra were recorded on a PerkinElmer LS 55 fluorescence spectrometer (PerkinElmer, Santa Clara, CA, USA). High performance liquid chromatography was performed on a Shimadzu LC system (Shimadzu, Columbia, MD, USA) with a photodiode array (PDA) detector (SPD-M20A), a pump (LC-20AT), and an LC column (Eclipse plus C18, 3.5 μm, 4.6 × 100 mm, Agilent, Santa Clarra, CA, USA). Gradient method was adopted using acetonitrile and 0.1% TFA-H_2O as mobile phase. The synthesis of EG_3Glu amino acid and the corresponding NCAs were reported previously.[21]

Synthesis of EG_3Glu

To a suspension of L-glutamic acid (1.0 g, 6.8 mmol) in triethylene glycol monomethyl ether (5 mL) cooled in an ice bath, sulfuric acid (1 mL) was added dropwise. The mixture turned into a viscous clear solution after being stirred at room temperature overnight. Following precipitation by a mixture of triethylamine (6 mL) and isopropanol (50 mL) twice, the obtained white solid was dissolved in DI water and lyophilized to yield a white solid of EG_3Glu (35% yield). ^{1}H NMR (500 MHz, δ, D_2O): 4.28 (t, 2H), 3.82–3.73 (m, 3H), 3.72–3.65 (m, 6H), 3.64–3.59 (m, 2H), 3.37 (s, 3H), 2.69–2.49 (m, 2H), 2.25–2.06 (m, 2H).

Synthesis of EG_3Glu-NCA

EG_3Glu (600 mg, 2.4 mmol) was dried under vacuum for 2 h before the reaction and then suspended in anhydrous THF (10 mL). A phosgene solution in toluene (15 wt%, 3.4 mL, 2 equiv.) was added into the suspension cooled in an ice bath. The reaction was performed at 50 °C for 2 h. The solvent was then removed under vacuum. The resulting oily residue was dissolved in a minimal amount of DCM and precipitated in anhydrous hexane to yield the product as a brownish oil (~85% yield) which was used for polymerization without further purification. The ^{1}H NMR of the oily residue (500 MHz, δ, $CDCl_3$): 7.42–7.32 (br, 1H), 4.45 (t, 1H), 4.42–4.17 (m, 2H), 3.82–3.46 (m, 10H), 3.36 (s, 3H), 2.64–2.43 (m, 2H), 2.41–2.05 (m, 2H).

General procedure of polymerization of EG_3Glu-NCA

The PZLL initiator was prepared following literature procedures.[32] The stock solution of PZLL initiator (2 mM, 100 μL) and 18-C-6 (20 mM, 10 μL) in chloroform was diluted with chloroform (390 μL) and then the aqueous buffer of H_3BO_3/citric acid/H_3PO_4 (pH = 9.0, 20 μL) was added. The resulting mixture was emulsified with a probe sonicator (Fisherbrand, Model 705, Thermo Fisher Scientific, Waltham, MA, USA). Non-purified EG_3Glu-NCA (1 M, 20 μL, for $[M]_0/[I]_0$ = 100) was diluted with chloroform (480 μL). Non-purified NCA was washed twice by aqueous buffer (sequentially with pH = 3.0 and pH = 7.0). Then Polystyrene beads with amine functional groups (2 mg, 0.002 mmol of amine) was added and vortexed for 30 s to remove excessive acidic/electrophilic impurities. After the removal of the beads through filtration, the NCA solution was vacuum-dried to determine the amount of the NCA. The dried NCA was re-dissolved in chloroform (500 μL) and aqueous buffer (pH = 9.0, 100 μL) was added. The mixture was vortexed for 30 s and mixed with the water-in-oil emulsion containing PZLL initiators. The block copolypeptides were precipitated into hexane/ether (v : v = 1 : 1) mixed solvent. The final polymers were obtained as white solids (59–63% yields).

NCA stability test in water/oil biphasic system

EG_3Glu-NCA (6 mg, 0.019 mmol) was dissolved in $CHCl_3$ (1 mL). The solution was mixed with DI water (120 μL) and vortexed for 30 s. The mixture was centrifuged and the $CHCl_3$ phase (150 μL) isolated for FTIR tests. FTIR tests were performed 0 h, 0.5 h, and 2.5 h after the solution was mixed with DI water.

Nanoparticle formulation of PZLL-*b*-P(EG_3Glu)

Block copolypeptides were dissolved in DMF (10 mg mL^{-1}) and added to vigorously stirred DI water (water : DMF = 5 : 1, v/v) at a rate of 0.1 mL min^{-1} using a syringe pump. The mixture was stirred for 1 h and then dialyzed against DI water

for 4 h (MWCO = 1 kDa). The resulting dispersion of nanoparticles was used for further studies.

TEM sample preparation

TEM samples were prepared on carbon film on copper grids (200 mesh, Electron Microscopy Sciences, Hatfield, PA, USA). One drop (3 μL) of diluted nanoparticle suspension of block copolypeptides (0.1–0.5 mg mL^{-1}) was placed on the carbon side and let sit for 1 min. Filter paper was used to blot the remaining suspension. One drop (3 μL) of DI water was placed on the grid and was blotted after 30 s. For negative staining, one drop (3 μL) of ammonium molybdate aqueous solution (1 wt%) was placed on the grid and was blotted away after 30 s. The samples on grids were imaged using JEOL 2100 cryo TEM at 200 kV.

Cryo TEM sample preparation

Cryo-TEM samples were prepared on lacey carbon film supported copper grids (200 mesh) using Vitrobot (FEI, Hillsboro, OR, USA). One drop (~3 μL) of diluted copolymer aqueous suspension (0.1–0.2 mg mL^{-1}) was placed on the grid, which was blotted with blotting paper. The sample residue was then vitrified by rapidly immersing it into liquid ethane. The vitrified sample was transferred to a JEOL 2100 cryo TEM microscope for imaging using a cryo-holder at 200 kV. The temperature of the sample was kept below −180 °C during sample preparation and imaging.

Formulation of drug-encapsulated nanoparticles

Diblock copolypeptides and PTX were dissolved in DMSO (10 mg mL^{-1} and 3 mg mL^{-1} for polymer and PTX, respectively) and added dropwise into DI water (water : DMSO = 10 : 1, v/v) using a syringe pump (0.1 mL min^{-1}). The mixture was vigorously stirred for 1 h and subjected to microtip sonication for 3 min. The resulting suspension was centrifuged (1000 rpm, 5 min) to remove unloaded PTX. The aqueous phase was then dialyzed against DI water for 24 h (MWCO = 3.5 kDa). The loading content was determined by HPLC.

Drug release study

PTX-loaded nanoparticle (0.4 mL, PTX 0.8 mg mL^{-1}) was placed into dialysis tubes (MWCO = 3.5 kDa) and immersed in DI water (35 mL) with 0.1% (v/v) Tween 80 at 37 °C for 24 h with stirring rate of 100 rpm. At each time intervals, an aliquot of the solution outside the dialysis bad (2 mL) was removed and lyophilized, followed by the addition of fresh DI water (2 mL) back. The PTX content was assayed using HPLC. Tests were performed in triplets.

Conclusions

In summary, we have successfully prepared oligo(ethylene glycol)-functionalized polypeptides from the ring-opening polymerization of non-purified EG_3Glu-NCA through a biphasic polymerization strategy. This strategy circumvented the needs for complicated anhydrous chromatography purification of EG_3Glu-NCA in high purity, which was absolutely essential to monophasic solution polymerization. High quality OEG-functionalized polypeptides with good yields (>50%) can be easily synthesized starting with non-purified, brownish OEG NCAs directly from the phosgenation of OEG functionalized amino acids. Coupled with the use of helical polypeptide with terminal amine as the initiator and crown ether as the catalyst which collectively enabled fast polymerization kinetics, the *in situ* purified "dirty" OEG NCAs were successfully used in the preparation of block copolypeptides with up to four polypeptide blocks. The prepared amphiphilic block copolypeptides can be used to prepare drug-containing nanoparticles with good drug loading, sub-100 nm nanoparticle size with low size dispersity, great stability in serum, and excellent capability preserving the encapsulated drugs with negligible drug release in solution. The biphasic polymerization procedures offer a facile method for even non-experts to prepare OEG-functionalized polypeptide material in a reproducible manner, which does not require extensive experience in NCA chemistry and access to sophisticated apparatus for NCA purification and polymerization (*e.g.*, Schlenk lines and glovebox). We believe this work will greatly expand the use of this class of unique, OEG-functionalized polypeptide materials.

Conflicts of interest

There are no conflicts to declare.

Acknowledgements

The research was supported by the U.S. National Science Foundation (CHE-1905097) and National Institutes of Health (1DP2EB024377-01).

References

1 T. J. Deming, *Chem. Rev.*, 2016, **116**, 786–808.
2 A. Rosler, G. W. M. Vandermeulen and H. A. Klok, *Adv. Drug Delivery Rev.*, 2012, **64**, 270–279.
3 B. Jeong, Y. H. Bae, D. S. Lee and S. W. Kim, *Nature*, 1997, **388**, 860–862.
4 C. Meng, Y. Cao, L. Sun, Y. Liu, G. Kang, W. Ma, J. Peng, K. Deng, L. Ma and H. Wei, *Biomater. Sci.*, 2020, **8**, 4206–4215.
5 Y. Mai and A. Eisenberg, *Chem. Soc. Rev.*, 2012, **41**, 5969–5985.
6 G. Riess, *Prog. Polym. Sci.*, 2003, **28**, 1107–1170.
7 B. Zhang, M. Li, M. Lin, X. Yang and J. Sun, *Biomater. Sci.*, 2020, **8**, 6969–6977.
8 C. He, S. W. Kim and D. S. Lee, *J. Controlled Release*, 2008, **127**, 189–207.
9 J. Zhu, *Biomaterials*, 2010, **31**, 4639–4656.

10 S. Xin, D. Chimene, J. E. Garza, A. K. Gaharwar and D. L. Alge, *Biomater. Sci.*, 2019, **7**, 1179–1187.
11 Z. Song, H. Fu, R. Wang, L. A. Pacheco, X. Wang, Y. Lin and J. Cheng, *Chem. Soc. Rev.*, 2018, **47**, 7401–7425.
12 C. Bonduelle, *Polym. Chem.*, 2018, **9**, 1517–1529.
13 C. Zhang, J. Yuan, J. Lu, Y. Hou, W. Xiong and H. Lu, *Biomaterials*, 2018, **178**, 728–737.
14 J. Wang, M. I. Gibson, R. Barbey, S. J. Xiao and H. A. Klok, *Macromol. Rapid Commun.*, 2009, **30**, 845–850.
15 Y. Hou, Y. Zhou, H. Wang, J. Sun, R. Wang, K. Sheng, J. Yuan, Y. Hu, Y. Chao, Z. Liu and H. Lu, *ACS Cent. Sci.*, 2019, **5**, 229–236.
16 X. Fu, Y. Shen, W. Fu and Z. Li, *Macromolecules*, 2013, **46**, 3753–3760.
17 S. Zhang, D. J. Alvarez, M. V. Sofroniew and T. J. Deming, *Biomacromolecules*, 2015, **16**, 1331–1340.
18 E. G. Gharakhanian and T. J. Deming, *J. Phys. Chem. B*, 2016, **120**, 6096–6101.
19 S. Zhang, W. Fu and Z. Li, *Polym. Chem.*, 2014, **5**, 3346–3351.
20 M. Yu, A. P. Nowak, T. J. Deming and D. J. Pochan, *J. Am. Chem. Soc.*, 1999, **121**, 12210–12211.
21 C. Chen, Z. Wang and Z. Li, *Biomacromolecules*, 2011, **12**, 2859–2863.
22 J. Shen, C. Chen, W. Fu, L. Shi and Z. Li, *Langmuir*, 2013, **29**, 6271–6278.
23 A. S. Abu Lila, H. Kiwada and T. Ishida, *J. Controlled Release*, 2013, **172**, 38–47.
24 P. Zhang, F. Sun, S. Liu and S. Jiang, *J. Controlled Release*, 2016, **244**, 184–193.
25 Z. Song, Z. Tan and J. Cheng, *Macromolecules*, 2019, **52**, 8521–8539.
26 Y. Liu, D. Li, J. Ding and X. Chen, *Chin. Chem. Lett.*, 2020, **31**, 3001–3014.
27 H. R. Kricheldorf, *Angew. Chem., Int. Ed.*, 2006, **45**, 5752–5784.
28 J. R. Kramer and T. J. Deming, *Biomacromolecules*, 2010, **11**, 3668–3672.
29 S. Trobro and J. Aqvist, *Proc. Natl. Acad. Sci. U. S. A.*, 2005, **102**, 12395–12400.
30 M. Beringer and M. V. Rodnina, *Mol. Cell*, 2007, **26**, 311–321.
31 D. A. Kingery, E. Pfund, R. M. Voorhees, K. Okuda, I. Wohlgemuth, D. E. Kitchen, M. V. Rodnina and S. A. Strobel, *Chem. Biol.*, 2008, **15**, 493–500.
32 Z. Song, H. Fu, J. Wang, J. Hui, T. Xue, L. A. Pacheco, H. Yan, R. Baumgartner, Z. Wang, Y. Xia, X. Wang, L. Yin, C. Chen, J. Rodriguez-Lopez, A. L. Ferguson, Y. Lin and J. Cheng, *Proc. Natl. Acad. Sci. U. S. A.*, 2019, **116**, 10658–10663.
33 Y. Xia, Z. Song, Z. Tan, T. Xue, S. Wei, L. Zhu, Y. Yang, H. Fu, Y. Jiang, Y. Lin, Y. Lu, A. L. Ferguson and J. Cheng, *Nat. Commun.*, 2021, **12**, 732.
34 Z. Song, H. Fu, R. Baumgartner, L. Zhu, K.-C. Shih, Y. Xia, X. Zheng, L. Yin, C. Chipot, Y. Lin and J. Cheng, *Nat. Commun.*, 2019, **10**, 5470.
35 X. Wang, Z. Song, Z. Tan, L. Zhu, T. Xue, S. Lv, Z. Fu, X. Zheng, J. Ren and J. Cheng, *ACS Macro Lett.*, 2019, **8**, 1517–1521.
36 J. Cheng, B. A. Teply, I. Sherifi, J. Sung, G. Luther, F. X. Gu, E. Levy-Nissenbaum, A. F. Radovic-Moreno, R. Langer and O. C. Farokhzad, *Biomaterials*, 2007, **28**, 869–876.
37 K. Rausch, A. Reuter, K. Fischer and M. Schmidt, *Biomacromolecules*, 2010, **11**, 2836–2839.
38 R. Tong and J. Cheng, *Polym. Rev.*, 2007, **47**, 345–381.
39 L. Tang, X. Yang, Q. Yin, K. Cai, H. Wang, I. Chaudhury, C. Yao, Q. Zhou, M. Kwon, J. A. Hartman, I. T. Dobrucki, L. W. Dobrucki, L. B. Borst, S. Lezmi, W. G. Helferich, A. L. Ferguson, T. M. Fan and J. Cheng, *Proc. Natl. Acad. Sci. U. S. A.*, 2014, **111**, 15344–15349.
40 Y.-Y. Huang, T.-W. Chung and T.-W. Tzeng, *Int. J. Pharm.*, 1999, **182**, 93–100.